Journal of the European Ceramic Society **15** (1995) 887–898

0955-2219/95/$9.50
0955-2219(95)00062-3

Analysis of the Isothermal Forced Flow Chemical Vapour Infiltration Process. Part II: Experimental Study

Y. G. Roman,[a] M. H. J. M. de Croon[b] & R. Metselaar[a]

[a]TNO, Centre for Technical Ceramics, PO Box 595, 5600 AN Eindhoven, The Netherlands
[b]Eindhoven University of Technology, Department of Chemical Engineering, PO Box 513, 5600 MB Eindhoven, The Netherlands

(Received 24 June 1994; revised version received 2 March 1995; accepted 10 March 1995)

Abstract

The preparation of homogeneously dense fibre reinforced SiC composites in a rapid way was the main objective of this study. Furthermore, densification should proceed as fast as possible. In Part 1 of this study,[1] some theoretical concepts were proposed of the infiltration mechanisms. The simple model was verified qualitatively using the results of experiments as is reported in this manuscript. Model and experiments do generally coincide. The trends predicted and found experimentally during alteration of the process or microstructural conditions appear to justify the theoretical concepts. Optimum infiltration conditions to gain largest density gain in the shortest time frame are 1320 K, outlet pressure of 6·65 kPa, total gas flow rate of 4 × 10^{-5} m^3 s^{-1}, MTS fraction of 16 vol% and pressure shut off point of 10 kPa.

1 Introduction

This paper is the continuation of the study to find the optimum process and microstructural conditions to gain high density ceramic composites using the Isothermal Forced Flow Chemical Vapour Infiltration (IFCVI) technique. In the previous paper, a simple mechanistic model was presented. In this manuscript the results are presented of an experimental study to verify the derived concept of the first paper.

2 Experimental Details

During the IFCVI of a porous carbon fibre preform, a CVD reaction takes place on the hot fibre surface. In this study, methyl-trichlorosilane (MTS) was used as both the silicon and carbon donor for the silicon carbide matrix. In the presence of a large amount of hydrogen it is known to form stoichiometric SiC.[2] The CVD reaction is:

$$CH_3SiCl_{3(g)} + H_{2(g)} \rightarrow SiC_{(s)} + 3HCl_{(g)} + H_{2(g)} \quad (1)$$

Raw materials

Disc shaped substrates with a diameter of 80 mm and a thickness of approximately 3 mm are used for the infiltration experiments. They were manufactured at DASA Aerospace,[3] Germany. They consist of Torayca T-300 (3K) fibres in plain woven layers that are stacked upon each other in a 0/90° orientation and woven together through a tow in the z direction. This orthogonally woven preform thus contains fibres in a 3D configuration.

Since the preform is very sensitive to handling and has a low stiffness, it is prefixed through impregnation with an alkali free liquid phenolic resin and compressed. After pyrolysis of the resin, the plates are cut into discs of 80 mm diameter using a water cutting machine. The carbon fibre content of the preforms varied from approximately 40–55 vol.% with respective thicknesses of 3·2–2·5 mm.

Infiltration experiments

Before infiltration, the preform plate is washed ultrasonically in acetone for 15 min and then positioned on top of a graphite support ring into a graphite holder. This holder is placed on top of a graphite injector tube through which the gases enter the holder and after flowing through the preform mainly axially, exit via the exhaust tube and pump (see Fig. 1). The graphite injector and holder are situated in a vacuum tight reactor chamber which is kept at a constant pressure and temperature by external resistance heating. This reactor is checked for leaks prior to each run. The preform is heated under a flow of nitrogen to 1200 K overnight at a rate of 120 $K.hr^{-1}$ and thereafter ramped to process temperature. After temperature stabilisation of at least 30 min, the process is started through introduction of the CVI gases at the process pressure.

The preform temperature is monitored by a thermocouple that is located in the bottom of the holder. All process settings (temperatures,

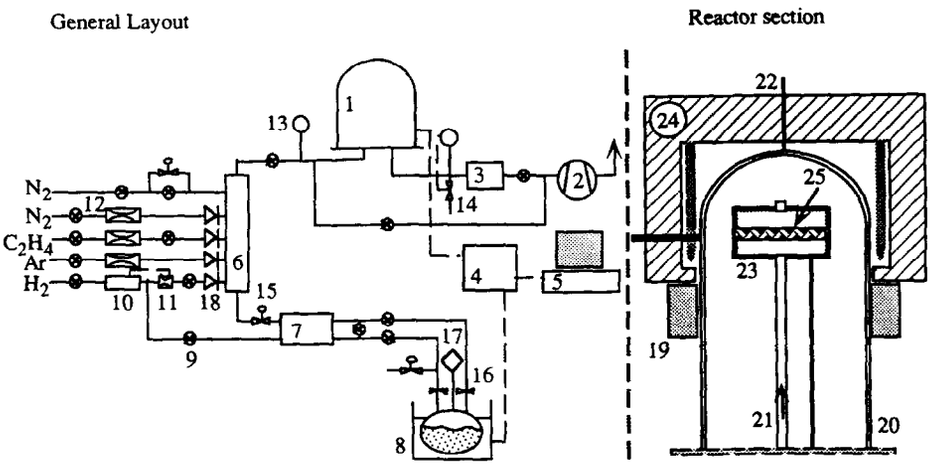

Fig. 1. A schematic layout of the FCVI reactor system; 1. bell jar reactor; 2. pump; 3. particle trap; 4. digital process and temperature controller; 5. P.C. data logger; 6. gas mixing box; 7. vapour source controller; 8. temperature controlled MTS bubbler; 9. pneumatic valve; 10. mass flow meter; 11. controller device of mass flow meter; 12. mass flow controller; 13. pressure gauge; 14. automatic nitrogen injection; 15. manual needle valve; 16. manual valve; 17. vacuum manometer; 18. check valve; 19. alumina wool; 20. alumina bell jar; 21. gas injector pipe; 22. thermocouple; 23. graphite preform holder; 24. furnace, 25. preform.

pressures, gas flows) during the infiltration are monitored by a data logging system attached to the FCVI apparatus which logs at 5 min intervals.

The methyltrichlorosilane (MTS) precursor flow rate is controlled by a vapour source controller. The MTS bubbler is weighed before and after each run to check the MTS flow rate. The 'weighed' MTS flow is used as the actual MTS flow value. The total amount of hydrogen gas, (i.e. the carrier gas for the bubbler and the bypass) is kept constant during the entire infiltration duration and additional argon is added for obtaining both a constant H_2/MTS ratio and total gas flow rate. The pressures at the injector and outlet side are monitored with two baratrons.

The pressure in the outlet is maintained at a constant value during the entire infiltration experiment. When the pressure in the injector at the start and the pressure at the end exceeds a certain shut off value, the infiltration is terminated and the gas flows are shut off. The preform is cooled to room temperature at 120 $K.hr^{-1}$ under a flow of argon.

In Table 1, the standard IFCVI process conditions are summarised.

Table 1. Standard IFCVI process conditions

Preform temperature (K)	1273
Outlet pressure (kPa)	6·65
MTS bubbler temperature (K)	288
Total gas flow rate (slm)	1
H_2 fraction at inlet (vol.%)	54
Ar fraction at inlet (vol.%)	37
MTS fraction at inlet (vol.%)	9
H_2/MTS ratio at inlet	6
Shut off pressure difference (kPa)	9·44 or 26·6

3 Characterization of the Preform

Raw preform

The outer dimensions and the weight of the disc shaped carbon fibre substrates with an initial diameter of 80 mm and a thickness of approximately 3 mm were measured before and after each run respectively with vernier callipers and an analytical balance. For the calculation of the fibre content V_f (volume fraction) of the preform relation[2] was used in which the small amount of pyrolised resin was neglected.

$$V_f = \frac{M_{preform}}{V_{preform}\,\rho_C} \tag{2}$$

Here, $M_{preform}$ (kg) is the mass of the raw preform and $V_{preform}$ is the volume of the raw preform disc in m^3 and ρ_C is the density of the carbon fibre ($1{\cdot}75 \times 10^3$ $kg.m^{-3}$).

Hereafter, the theoretical ideal density ρ_i ($kg.m^{-3}$) of a densified preform where the total pore volume is completely filled with silicon carbide matrix material ($\rho_m = 3{\cdot}2 \times 10^3$ $kg.m^{-3}$) can be calculated according to:

$$\rho_i = V_f\,\rho_c + (1 - V_f)\,\rho_m \tag{3}$$

The initial deposition area A_{dep} (m^2) is the weight $M_{preform}$ (kg) of the raw preform multiplied by the specific surface area S_C ($m^2.kg^{-1}$) of the carbon fibres (550 $m^2.kg^{-1}$). Assuming that there is no trapped porosity:

$$A_{dep} = S_C M_{preform} \tag{4}$$

Permeability

The preform permeability K, is defined as the conductance of the preform for the gas flow. The

initial permeability of the raw preform is dependent on its microstructure only and thus dependent on its fibre content. The gas permeability K_g (m^2) of a porous structure is given by Darcy's law as:[4]

$$K_g = \frac{uo\ \mu\ L}{\Delta p} \tag{5}$$

where L is the preform thickness (m), uo is the average superficial gas velocity ($m.s^{-1}$), μ is the dynamic gas viscosity (Pa.s) and ΔP is the pressure difference across the preform plate (Pa). This form of Darcy's law has, however, a very narrow range of validity.[5]

The permeability of a porous system is supposed to be a constant by definition. In case the fluid is an incompressible liquid and inertial effects can be neglected,[6] K is indeed a constant. In the case of gases, especially at low total pressure, the fluid does not always stick to the wall of the pores as required in Darcy's law (Poiseuille type flow) and a phenomenon termed 'slip' can occur. This slipping of the fluid along the pore walls gives rise to an apparent dependence of permeability on pressure. This dependence is called the Klinkenberg effect and occurs typically at low total pressure and corresponding Knudsen numbers[7] between 0·1 and 1.

Because the gas permeability is thus dependent on the pressure (drop) and not solely a microstructural constant, for the sake of comparison within the range of a process condition, it is necessary to express the evolution of the preform microstructure during CVI in other parameters like porosity, pore size, fibre diameter, fibre arrangement and wall thickness and to be more complete also in terms of tortuosity. Still, the permeability of the raw preforms is measured as a function of fibre content (and preform thickness), outlet pressure and total gas flow rate to obtain an order of magnitude of the conductance to gas flow. Hereto, argon gas flowed through the raw preform in the IFCVI apparatus at a temperature of 1273 K. The argon flow rate was varied stepwise from 0 to 2 slm at 2·66, 6·65 and 9·31 kPa outlet pressure and the pressure drop across the preform plate was measured using two matched pressure gauges.

Dimensionless numbers

The Peclet and the first Damköhler numbers can aid in the description of the IFCVI process conditions that were used for the experiments. These are defined in Part 1 of this study for a hollow cylindrical pore. For a more realistic definition of the preform the following definitions[9] were applied that are indicative for the raw preform and process conditions at $t = 0$.

$$Pe_{bed} = \frac{u d_f\ \tau^2}{\epsilon\ (1 - \epsilon)\ D_{multi}} \tag{6}$$

$$DaI_{bed} = \frac{4\ k_s\ \epsilon}{\tau\ u} \tag{7}$$

with τ (–) is the tortuosity of the preform and assumed to equal 2, k_s ($m.s^{-1}$) is the first order reaction rate coefficient, ϵ (vol. fraction) is the raw preform porosity, d_f (m) is the fiber diameter = 7×10^{-6} m, D_{multi} ($m^2.s^{-1}$) is the multi component diffusion coefficient.

Infiltrated preform

After the infiltration experiments, the composite discs were weighed to calculate the overall MTS conversion or total yield of MTS: η in the preform into solid matrix material. This η (%) is estimated by:

$$\eta = \frac{M_{m,dep}}{M_{m,max}} \times 100 \tag{8}$$

where $M_{m,dep}$ (kg) is the total deposited mass of matrix material and $M_{m,max}$ (kg) is the mass of matrix material that would be deposited at a complete conversion of MTS. Note that (reaction 1) 1 mol of MTS yields 1 mol of SiC.

This definition of η is very similar to Δ (eqn 5 part 1), whereas the first represents the conversion based upon the whole preform volume and the latter one represents the conversion across the length of a cylinder pore. This similarity implies that large η will yield low composite density due to low uniformity of the deposited matrix in axial direction.

After weighing of the composite preforms, they were cut into bars. Out of each disc, four samples from the middle section were cut, with typical dimensions of $60 \times 10 \times 3$ mm^3 using a diamond blade. The bars were ultrasonically cleaned in ethanol for 15 min and dried at 400 K for at least one night. Since the samples absorb moisture from the air, each bar was weighed directly after drying on an analytical balance. The outer dimensions of each bar were measured with callipers and the percentage of the ideal density expressed as the relative bulk composite density $\rho_{b\ rel}$ (vol.%) was estimated through:

$$\rho_{b\ rel} = \frac{M_b}{V_b\ \rho_i} \times 100 \tag{9}$$

with V_b (m^3) being the bulk volume of the bar and M_b (kg) the weight of the infiltrated bar. The arithmetic mean of the relative density of the four bars indicates the $\rho_{b\ rel}$ of each preform disc.

Analysis of the matrix composition

For the determination of the phase structure of the deposited matrix material, XRD analysis was

used with CuKα radiation at 35 kV and a 2θ diffraction angle between 20 and 80°. The SiC matrix was further analysed using a microprobe (EPMA, Jeol type JXA-8600SX). The composition of the matrix as a function of infiltration temperature, i.e. the silicon, carbon and oxygen content were measured quantitatively using an acceleration voltage of 10 kV. Both sides of the composite discs were measured *viz.* the gas inlet side and gas outlet side.

4 Results and Discussion

The effect of the different process variables such as preform temperature, total gas flow rate, MTS fraction in the inlet gas mixture and the outlet pressure on the infiltration time and composite density was studied. Furthermore, the effect of the fibre content and the densification stage (pressure drop) as a function of infiltration time are presented.

First, the reproducibility of the process and of the characterization methods are tested.

Reproducibility

A blank run was performed in which a preform plate was heated up to the typical process temperature of 1273 K and subjected to a mixture of H_2 and Ar, at a rate of respectively 500 and 100 sccm for 5 h. After cooling according to the normal procedure, the preform dimensions and weight were checked. No significant difference in weight or volume was detected.

So, it can be concluded that the changes of the preform, described hereafter, are solely the consequence of the infiltration procedure.

Before the effect of any process variable was tested, the reproducibility of the IFCVI process was estimated by carrying out twice, three repeated runs, (i.e. three runs under the same conditions). The relative bulk density (average of four bars out of one sample, $n = 4$) varied 0·5%, whereas it varied more when measured with a whole composite disc ($n = 1$), i.e. 2·2%. The latter error is larger, because of the error that is made in the measurement of the composite thickness, due to a radial thickness gradient of the deposited coating on the gas inlet side of the sample of approximately 10%.

Process conditions during the run

The data logging system allows continuous monitoring of the process settings. A typical result is given in Fig. 2. The total hydrogen flow rate is the summation of the hydrogen flow rate through the bubbler and the 'back up' hydrogen flow rate that is added additionally. All process conditions

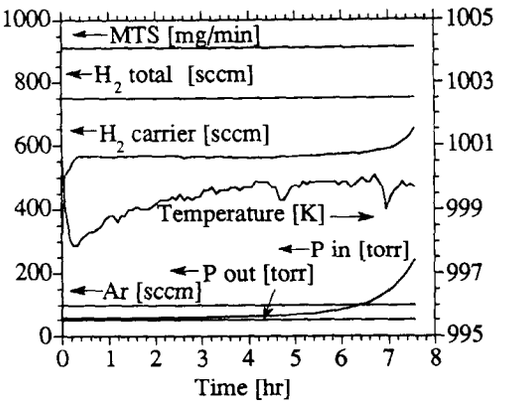

Fig. 2. The process conditions as a function of infiltration time as monitored with the data logging system. 'H_2 carrier' is the H_2 flow through the MTS bubbler. It increases due to increase in injector pressure 'pin'.

remain constant during the run with the exception of the injector pressure. Temperature typically varies ±2 K.

Pressure difference shut off point

During the infiltration process the gas permeability of the preform decreases due to the deposition of the SiC on the pore walls. Consequently, the pressure drop across the preform starts to rise. For comparison of the preforms after the infiltration process and especially of the infiltration time, a shut off point is required.

Therefore, the pressure drop across the preform is used as the shut off quantity and despite changing the process conditions it is kept at a constant shut off value. Its definition is:

$$\Delta p_{\text{shut off}} = (p0_{t=\text{end}} - p0_{t=0}) \qquad (10)$$

For the bulk density estimation, the average of the four bars, cut from the middle section of the composite disc were used, thus $n = 4$. The printed dots in the plots presented hereafter, are the arithmetic means of the relative densities of the four bars from one experiment and the error bars are indicative of the 95% confidence interval, assuming that the data is normally distributed.

Axial uniformity

It is clear that within the goal of achieving homogeneous composite density, the axial gradient of the SiC deposition within the preform plays an important role. The direct quantitative measurement of the uniformity in axial direction with the purpose of comparison of the samples, appeared however to be impossible for these thin samples.

Therefore, the simplest method was used, which is the estimation of the overall bulk density by eqn 9. Due to the fact that the (theoretical) density of the SiC matrix is larger than of the composite

material C/SiC, the relative bulk density of a composite with a thick SiC coating on the gas inlet side will be lower compared to one with a thin layer, assuming that the C/SiC composites without the thin layer have the same density. The relative bulk density is therefore not only a tool for measuring density but in a sense for homogeneity as well.

4.1 Effect of the total gas flow rate

Matrix composition at high flow rate

It was noticed that at high total gas flow rate, (i.e. >1·8 slm) the deposited SiC layer on the gas inlet side had a black appearance. The coatings produced at low gas flow rate had a shiny silvery appearance. The composition of the black deposit was measured using EPMA at an acceleration voltage of 6 kV. Although oxygen free, the Si/C ratio was in the order of 1·5, (i.e. 20 at.% free silicon). It is anticipated that the silicon forms more easily as compared with carbon at this high gas velocity.

Infiltration behaviour

From Fig. 3, it is evident that increase of the total gas flow rate results in a decrease of the infiltration time. As in CVD, it is anticipated that at low total gas flow rates, mass transport limitations— either convective or diffusive — are dominating growth. For clarification, if either convective or diffusive mass transport has been dominating matrix growth, the following concepts were audited.

During FCVI processing, the gas flows through the pores. The transport of the species is driven by convection. A boundary layer develops along the wall of the pores through which diffusive mass transport (low Peclet number) of the gas species occurs.

Consequently,[1] t_i is proportional to the reciprocal of the square root of $Ft^{\#}$. On the other hand, if convection in the remaining pore cavity — surrounded by the boundary layer — is faster than diffusion (large Peclet number), the infiltration time is proportional to exp $(c \times Ft^{\#-1})$.

Unfortunately, on this basis it is not possible to distinguish which of the two transport mechanisms has controlled matrix growth. Therefore, the magnitude of the Peclet number should indicate if either diffusive or convective mass transport has taken place in the regime of low total gas flow rate. Since the calculated Peclet numbers for the packed bed at the process conditions used — indicated in the figure caption of Fig. 3 — are relatively large, i.e. larger than 10^{-3} *viz.* $3{\cdot}8 \times 10^{-3}$, it is assumed that forced convection has been more dominant than diffusion. At large gas flow rates, the growth is limited by the kinetics of the deposition reaction at the fibre surface and becomes independent of flow rate.

The transition between the two growth regimes in Fig. 3, e.g. mass transport (at large Damköhler numbers and low flow rates) towards kinetically controlled growth (at small Damköhler numbers and large flow rates) was estimated by the intersection of the two slopes of the curves of the growth regimes. Surface reaction limitation starts at a rate of approximately 0·8 slm and at a corresponding calculated DaI_{bed} number of approximately 0·06–0·05.

It is anticipated that the infiltration time will decrease until a minimum is reached asymptotically when the growth is totally kinetically controlled, whereas at very low flow rate (close to 0) the infiltration time will reach infinity. Although the error of the measurements presented in Fig. 4 is relatively large, it may be stated that there is an increasing trend in density as a function of total gas flow rate. At zero gas flow rate, beyond the scope of the fire, the bulk density equals the raw relative bulk density of the starting preform (typically 36·5%).

Large total gas flow rates are thus advantageous in achieving large bulk densities. This is not

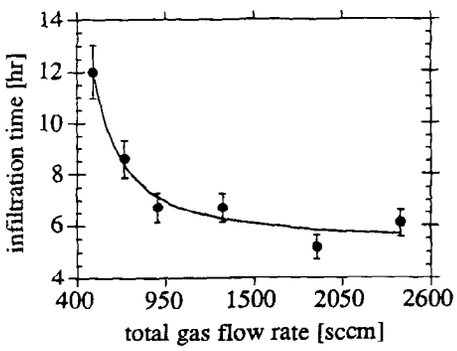

Fig. 3. The infiltration time versus total gas flow rate $Ft^{\#}$. T = 1273 K, H_2/MTS = 6·15, V_f = 51·2 vol%, $L = 2{\cdot}89 \times 10^{-3}$ m, p_L = 6·65 kPa, $\Delta p = 9{\cdot}44 \times 10^3$ Pa $Pe_{bed} = 3{\cdot}88 \times 10^{-3} - 2{\cdot}20 \times 10^{-2}$, $DaI_{bed} = 6{\cdot}81 \times 10^{-2} - 1{\cdot}74 \times 10^{-2}$.

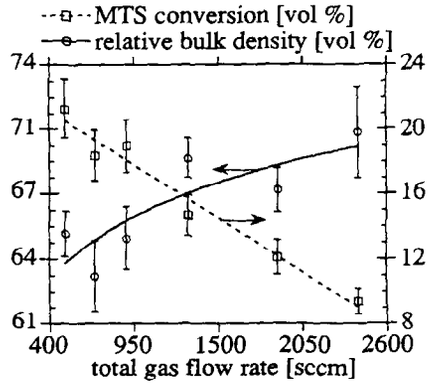

Fig. 4. The relative bulk density and MTS conversion versus total gas flow rate $Ft^{\#}$. T = 1273 K, H_2/MTS = 6·15, V_f = 51·2 vol%, L = 2·89 mm, p_L = 6·65 kPa, $Pe_{bed} = 3{\cdot}88 \times 10^{-3} - 2{\cdot}20 \times 10^{-2}$, $DaI_{bed} = 6{\cdot}81 \times 10^{-2} - 1{\cdot}74 \times 10^{2}$, $\Delta p = 9{\cdot}44 \times 10^3$ Pa.

surprising, considering the fact that through increase of flow rate, the gas velocity within the pores will increase and the uniformity of the matrix distribution will enlarge. At even larger flow rates, i.e. >0·8 slm (Fig. 3), the growth is limited by surface kinetics.

The enhancement of the matrix deposition uniformity is also demonstrated by the MTS conversion that decreases linearly with flow rate. Despite the fact that density is reaching a more or less constant value above 1·5 slm, the MTS conversion is still decreasing. This is explained as follows. During kinetically limited growth only a certain limited amount of molecules can be converted into solid matrix material. The numerator in eqn 8 ($M_{m,dep}$) will remain constant. Larger mass transfer fluxes will, however, increase the denominator $M_{m,max}$. The MTS conversion will decrease until the denominator reaches infinity.

At very large gas velocities, this phenomenon can reach an extreme. When the residence time t_r of the gas in the preform structure gets very short, the critical reaction time t_{cr} can become larger than the residence time of the gas. If so, the MTS has insufficient time to react. This explains the fact that in the centre part of the discs, infiltrated at flow rates exceeding 1·5 slm and/or at outlet pressures ≤1·33 kPa, poor deposition was achieved. The residence time of the gaseous species in the centre of the disc is based upon the Poiseuille gas velocity. On the axis of the preform $u_{bed,ax} = 2u_{bed}$. In general terms as $t_r < t_{cr}$ (s) deposition will be severely hindered and hence in the centre of the preform disc:

$$\frac{\epsilon L_{preform}}{2\,\tau\,uo} < \frac{1}{k_s \times av} \qquad (11)$$

where av is defined[1] as $4 \times d_f^{-1}$. Calculation of t_r and t_{cr} (with assumed tortuosity τ of 2) indicated that at mean gas bed velocities larger than 3 m.s^{-1} this phenomenon can occur.

During kinetically controlled growth, theoretically uniform deposition should occur. However, due to the pressure gradient across the preform, deposition will always be larger at the gas inlet side as compared to the outlet side. Therefore, complete homogeneity can never be reached using the IFCVI technique. Best uniformity can be gained at large flow rates when the process is just kinetically limited. At larger gas flow rates, beyond the scope of the plot, it is anticipated that density can decrease again if the MTS has insufficient time to react at the fibre surface, or due to the following phenomenon.

The pressure drop across the preform is a function of the square root of the total gas flow rate. Experiments performed at high total gas flow rate will consequently start at a high value of the inlet pressure. The corresponding SiC growth rate at the high pressure side will thus be much larger than the growth rate at the opposite side of the preform, i.e. $G_0 >> G_L$ ($t = 0$).

All experiments are finished at the same pressure drop value (eqn 10). Consequently the amount of uniformly deposited matrix will be larger when the flow rate is small ($G_0 \approx G_L$), resulting in a higher density. According to this consideration — that coincides with the model predictions of Part 1 of this study — the relative bulk density presented in Fig. 4 should reach a maximum at the point where growth is kinetically limited and the infiltration process begins at the condition that $p_0 \approx p_L$. These theoretical considerations could not experimentally be verified due to practical limitations. The p_0 over p_L ratio — as measured at the largest experimental flow rate — is 1·6 at the start of the infiltration process and is not sufficient to negatively affect the deposition uniformity.

4.2 Effect of the outlet pressure

In Fig. 5 the results are presented of the study on the effect of outlet pressure on the infiltration time. Increase of the outlet pressure results in decrease of the infiltration time in a non-linear way. It is known that the precursor concentration is a linear function of the total pressure. Increase in (outlet) pressure therefore results in a larger growth rate of the matrix.

The gas velocity is also affected by the total pressure. At low pressure, when the gas velocity is high, it is assumed that chemical kinetics control matrix growth. In the other regime at high total pressure, mass transport governs matrix growth and decrease in infiltration time is less severe.

On the other hand, when diffusive mass transport — across the boundary layer that is present along the pore wall — would control matrix growth, infiltration time would be independent of total pressure.

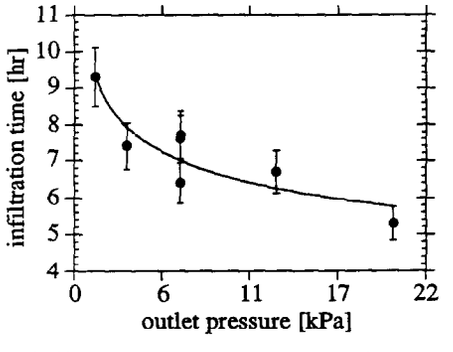

Fig. 5. The infiltration time versus total outlet pressure p_L. T = 1269 K, H_2/MTS = 4·97, V_f = 45·9 vol%, $L = 2{\cdot}96 \times 10^{-3}$ m, $Ft^{\#} = 1{\cdot}67 \times 10^{-5}$ m^3.s^{-1}, $Pe_{bed} = 5{\cdot}03 \times 10^{-3}$, $Dal_{bed} = 1{\cdot}17 \times 10^{-2} - 9{\cdot}50 \times 10^{-2}$, $\Delta p = 2{\cdot}66 \times 10^4$ Pa.

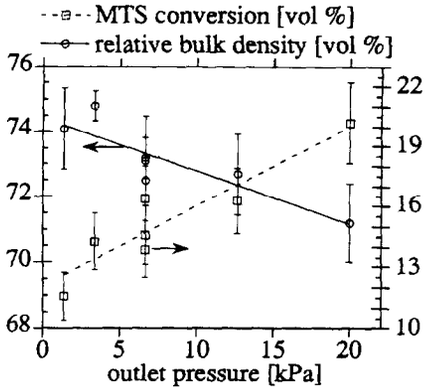

Fig. 6. The relative bulk density and MTS conversion versus total outlet pressure p_L. T = 1269 K, H_2/MTS = 4·97, V_f = 45·9 vol%, L = 2·96 × 10^{-3} m, $Ft^{\#}$ = 1·67 × 10^{-5} $m^3.s^{-1}$, Pe_{bed} = 5·03 × 10^{-3}, DaI_{bed} = 1·17 × 10^2 – 9·50 × 10^{-2}, Δp = 2·66 × 10^4 Pa.

Comparison of these theoretical concepts with the experimental results that are presented in Fig. 5, shows that convection has been the mass transport mechanism at the corresponding Peclet number of 5 × 10^{-3}.

In Fig. 6, the relative bulk density decreases with increasing outlet pressure. When the outlet pressure is increased — during convection controlled growth — the gas velocity through the pores will reduce and the uniformity of the matrix distribution is lowered. This results in a reduction of the relative bulk density and is also demonstrated by the increase in MTS conversion.

One may conclude that the experiments have predominantly been performed within the mass transport limited regime, since density and eventually MTS conversion would remain constant with pressure otherwise. From the effect of the total gas flow rate it is known that transition between the two growth regimes is in between a DaI_{bed} of 0·05 and 0·06. This implies that only the first three data points of the experiments in Fig. 6, have been performed at surface reaction limited conditions where the effect of outlet pressure on relative density is indeed negligible.

4.3 Effect of the preform temperature

Matrix composition

The composition of the SiC matrix of all preform discs on both gas inlet and outlet side were measured using EPMA. The coatings were oxygen and chlorine free, i.e. within the error of the detection limit. The SiC coating on the gas inlet side of all specimens had a shiny silvery appearance. The Si/C ratio varied slightly from 1·0 to 1·1 corresponding to a maximum free silicon content of 5 at.%. No effect of the SiC location (either gas inlet or outlet) was detected.

XRD measurements on both sides of the samples indicated that the coating was crystalline β-SiC and contained mainly cubic crystals. Traces of hexagonal SiC were observed at the gas inlet side of the preform.

Consequently, it is assumed that the density of the matrix material is independent of the deposition temperature and equal to the theoretical density of silicon carbide.

Infiltration behaviour

In Fig. 7 the infiltration time is presented as a function of preform temperature.

At high temperatures, matrix growth is fast. In accordance with theoretical considerations, the infiltration time reduces with increasing temperature due to the Arrhenius behaviour of the deposition reaction. Since the first Damköhler number is smaller than 0·054 within the whole range of experiments, it is anticipated that kinetics have been controlling the formation of SiC.

In Fig. 8 relative composite density is independent of temperature and possibly even positively affected by an increase of temperature. On the other hand, the MTS conversion is a linear increasing function of temperature.

The independence of the relative bulk density on temperature can be explained if chemical kinetics are governing matrix growth. This statement is

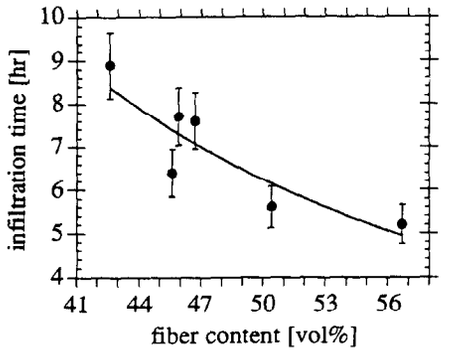

Fig. 7. The infiltration time versus preform temperature T. H_2/MTS = 4·98, V_f = 44·8 vol%, $Ft^{\#}$ = 1·67 × 10^{-5} $m^3.s^{-1}$, L = 3·06 × 10^{-3} m, p_L = 1·33 kPa, Pe_{bed} = 1·32 × 10^{-2}, Δp = 2·65 × 10^4 Pa, DaI_{bed} = 3·49 × 10^{-3} – 5·41 × 10^{-2}.

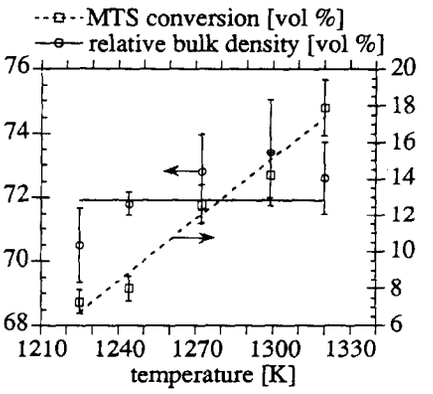

Fig. 8. The relative bulk density and MTS conversion versus preform temperature T. H_2/MTS = 4·98, V_f = 44·8 vol %, $Ft^{\#}$ = 1·67 × 10^{-5} $m^3.s^{-1}$, L = 3·06 × 10^{-3} m, p_L = 1·33 kPa, Pe_{bed} = 1·32 × 10^{-2}, Δp = 2·65 × 10^4 Pa, DaI_{bed} = 3·49 × 10^{-3} – 5·41 × 10^{-2}.

in accordance with the value of $DaI_{bed} < 0{\cdot}05$–$0{\cdot}06$. In general terms, at low temperature, SiC growth is kinetically controlled.

The relative bulk density will remain unaffected as long as the initial pressure gradient ($t = 0$) is not too large, (i.e. $G_0 \approx G_L$).

Depletion effect can be excluded and deposition is uniform. Hereafter, at higher temperatures, density will decrease because mass transport limitations dominate matrix growth and depletion of the MTS — that flows in axial direction through the pores — is rising and the resulting deposition profile is less uniform. At very high temperatures, when the MTS is almost completely depleted from the bulk gas stream, no SiC is deposited deeper into the preform. What remains is an only partially infiltrated preform.

4.4 Effect of the MTS fraction in the gas mixture

Experimental examination of the dependence of the infiltration time as a function of MTS fraction — shown in Fig. 9 — is in accordance with theoretical predictions (see Part 1 of this study). The concentration of the precursor is a linear function of its mole fraction in the gas mixture. The infiltration time is thus proportional with X_{MTS}^{-1}. The input fraction of the MTS has no effect on the resulting relative bulk density.

Theoretical concepts indicate that neither in the mass transport controlled regime nor during kinetically controlled growth is an effect of the MTS fraction on the composite density expected. In Fig. 10 this theory is experimentally verified for the kinetically controlled growth regime since DaI_{bed} is smaller than 0·05 for all experiments. This independence of MTS content in the gas mixture on the composite density is also confirmed by the fact that the first Damköhler number is independent of precursor concentration as long as first order reactions apply.

Depletion of the precursor is independent of absolute concentration and hence the relative density

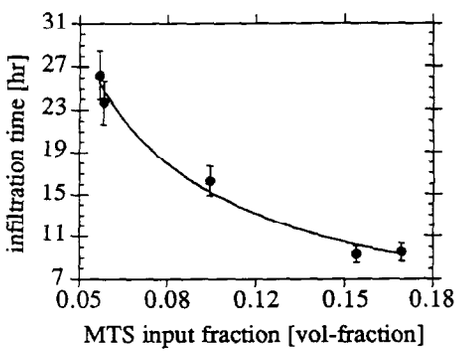

Fig. 9. The infiltration time versus input MTS fraction in the gas mixture x_{MTS}. $T = 1269$ K, $V_f = 44{\cdot}8$ vol%, $L = 3{\cdot}03 \times 10^{-3}$ m, $Ft^{\#} = 1{\cdot}67 \times 10^{-5}$ m^3 s^{-1}, $p_L = 1{\cdot}33$ kPa, $Pe_{bed} = 1{\cdot}33 \times 10^{-2} - 3{\cdot}57 \times 10^{-3}$, $DaI_{bed} = 1{\cdot}22 \times 10^{-2}$, $\Delta p = 2{\cdot}66 \times 10^4$ Pa.

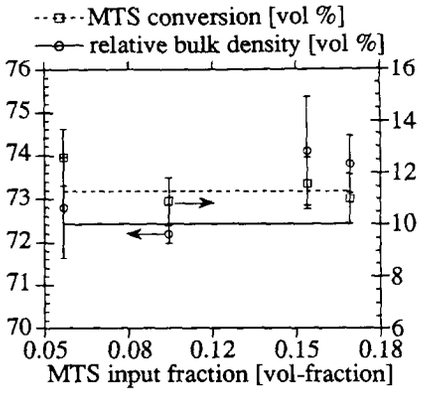

Fig. 10. The relative bulk density and MTS conversion versus input MTS fraction in the gasmixture x_{MTS}. $T = 1269$ K, $V_f = 44{\cdot}8$ vol%, $L = 3{\cdot}03 \times 10^{-3}$ m, $Ft^{\#} = 1{\cdot}67 \times 10^{-5}$ m^3.s^{-1}, $p_L = 1{\cdot}33$ kPa, $Pe_{bed} = 1{\cdot}33 \times 10^{-2} - 3{\cdot}57 \times 10^{-3}$, $DaI_{bed} = 1{\cdot}22 \times 10^{-2}$, $\Delta p = 2{\cdot}66 \times 10^4$ Pa.

is constant. Clearly, the MTS content should be sufficiently high to overcome almost complete conversion of the MTS before the gas has arrived at the other end of the preform.

4.5 Effect of the fibre content and preform thickness

Increase of the fibre content in the preform volume is achieved by exerting higher pressure on the preform during its prefixing stage, resulting in not only larger fibre content per volume (V_f), and tortuosity (τ), but also in lower thickness (L) and smaller average pore size (d_p). These quantities are measured and presented in Table 2 as a function of fibre content. It appears that even the surface area available for deposition (A_{dep}) is increased.

Due to these microstructural changes, the gas permeability of the porous structure K_g will also differ between the samples.

Permeability of the raw preform: experimentally and analytically

The gas permeability K_g (m^2) was measured as a function of raw preform fibre content, outlet pressure and argon flow rate at 1273 K. The details of the raw preforms used for the permeability test are given in Table 2.

The results can be fitted according to Darcy's law (eqn 5) for incompressible fluids, since for a constant outlet pressure, $uo\mu L$ follows a linear relationship with Δp and the slope represents K_g.

However, the data obtained at different outlet

Table 2. Raw preform characteristics for the permeability test at 1273 K under argon flow.

Exp no.	V_f (vol %)	Thickness (m)	A_{dep} (m^2)
52	42·6	$3{\cdot}17 \times 10^{-3}$	6·54
50	45·6	$2{\cdot}95 \times 10^{-3}$	6·66
53	49·4	$2{\cdot}74 \times 10^{-3}$	6·68
51	56·7	$2{\cdot}53 \times 10^{-3}$	6·94

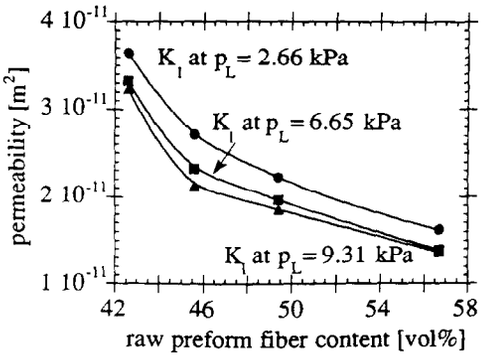

Fig. 11. The permeability K_l versus raw preform fibre content V_f and outlet pressure p_L at 1273 and argon flow.

pressures resulted in different slopes, so that K_g is a function of average pressure. Best fit was achieved with the permeability expression for compressible gas flow with slip.[1] It was found that the experimental data could not be fitted within the whole range of process variables and no complete elucidation of the proper permeability equation was gained. Deviations were noticed at the lowest outlet pressure of 6.65 kPa and are probably due to inertial effects.[7]

From Table 2 and Fig. 11 it can be concluded that permeability decreases with increasing fibre content, due to the less open structure.

Also, it was found that permeability at the low absolute total pressure conditions used, increases linearly with decreasing outlet pressure or increasing pressure drop.

A constraint for proper infiltration is the fact that sufficiently high permeabilities are required to overcome excessive inlet pressures (or Δp) so that infiltration can proceed sufficiently long to be able to grow matrix into the structure. More generally stated, $LA^{-1}K^{-1}$ should be small (eqn 5) with A representing the cross flow area (m^2).

Infiltration behaviour

As illustrated in Fig. 12, when the fibre content of the raw preform is increased, the infiltration time

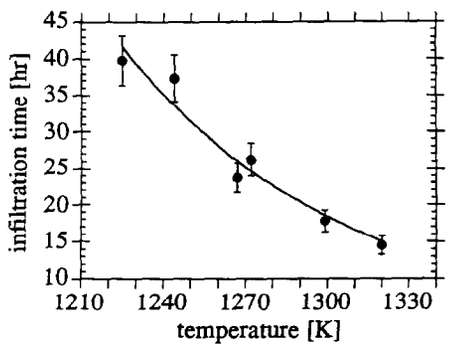

Fig. 12. The infiltration time versus raw preform fibre content. T = 1271 K, H_2/MTS = 5·02, V_f = 42·6–56·7 vol%, $Ft^{\#}$ = 1·67 × 10^{-5} $m^3.s^{-1}$, L = 3·17 × 10^{-3}–2·96 × 10^{-3} m, Pe_{bed} = 5·05 × 10^{-3}, DaI_{bed} = 3·97 × 10^{-2}–3·32 × 10^{-2}, A_{dep} = 6·54–6·94 m^2, Δp = 2·65 × 10^4 Pa.

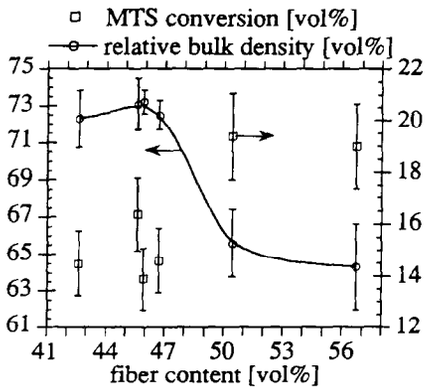

Fig. 13. The relative bulk density and MTS conversion versus raw preform fibre content. T = 1271 K, H_2/MTS = 5·02, V_f = 42·6–56·7 vol%, $Ft^{\#}$ = 1·67 × 10^{-5} $m^3.s^{-1}$, L = 3·17 × 10^{-3}–2·96 × 10^{-3} m, Pe_{bed} = 5·05 × 10^{-3}, DaI_{bed} = 3·97 × 10^{-2}–3·32 × 10^{-2}, A_{dep} = 6·54–6·94 m^2, Δp = 2·65 × 10^4 Pa.

is reduced. Yet, the variation of the raw preform fibre content is a combined effect of more than only one variable. Pore size is reduced, whereas the surface area and tortuosity of the structure is increased (Table 2). So, the filling of the pores is relatively fast at large fibre content. This effect is mainly due to the small pore diameter of the preform of high fibre content.

The relative bulk density of the composite is a decreasing function of the fibre content and is presented in Fig. 13. Apparently, the deposition uniformity is enhanced when V_f is decreased. This effect cannot be explained in terms of decreasing τ or A_{dep} or increasing L, but only in increasing pore diameter d_p.

The pore gas velocity that controls the uniformity of the matrix distribution along the pore axis is a positive function of the pore diameter (eqn 13, Part 1 of this study). And since the mean pore diameter is a decreasing function of the fibre content, the density will thus decrease with increasing V_f.

For achieving the same composite density, a preform with low fibre content and high permeability should be infiltrated up to a lower pressure shut off point as compared with a preform of high fibre content and low permeability. An optimum in density gain, i.e. the largest density in the shortest time is reached at a fibre content of 46 vol.%.

4.6 Apparent reaction rate equation

Introduction

Premature homogeneous decomposition[8] of MTS in the gas phase in front of the preform can rule the kinetic equation. Therefore, the amount of decomposed MTS in the gas phase prior to and in the preform was calculated and appeared to be smaller than 10% for all experiments.[1] It is

therefore assumed that the kinetic equation derived in the following, is caused by the direct reaction of MTS to SiC without prior decomposition.

Experimental results

The overall apparent reaction rate equation within the porous structure that relates the infiltration time with the process conditions within the regime of kinetically controlled growth was quantified. The results of the effect of temperature (Section 4.3) and MTS fraction in the gas mixture (Section 4.4) were used for the estimation of the overall apparent reaction rate equation. First, the activation energy (E_a) of the surface reaction was derived from plotting the logarithm of the matrix growth rate versus the reciprocal temperature in Fig. 14(a).

The matrix growth G_{SiC} (mol.m^{-2} s^{-1}) is calculated according to:

$$G_{SiC} = \frac{M_{m,dep}}{m_{SiC} A_{dep} t_i} \tag{12}$$

where $M_{m,dep}$ (kg) is the weight increase of the preform due to SiC deposition, m_{SiC} is the molar mass of SiC (kg.mole^{-1}), A_{dep} (m^2) is the deposition area (eqn 4) and t_i (s) is the infiltration time. The slope of the plot Fig. 14(a) represents $-E_a/R_g$, from which an apparent activation energy of 135 kJ.mol^{-1} was calculated. The experiments where the MTS input fraction was varied, were used for the estimation of the partial reaction order and pre-exponential factor. In Fig. 14(b) it is demonstrated that the SiC matrix growth follows a first order dependence in MTS.

The slope of the plot equals the partial reaction order, whereas the intercept represents $\ln(k_s)$. From k_s (m.s^{-1}) and the activation energy, k_0 is calculated to equal 16·45 m.s^{-1}.

This results in the overall apparent reaction equation for the silicon carbide growth rate G_{SiC} (mol.m^{-2}.s^{-1}) within a porous structure using MTS in an excess of H_2 and Ar:

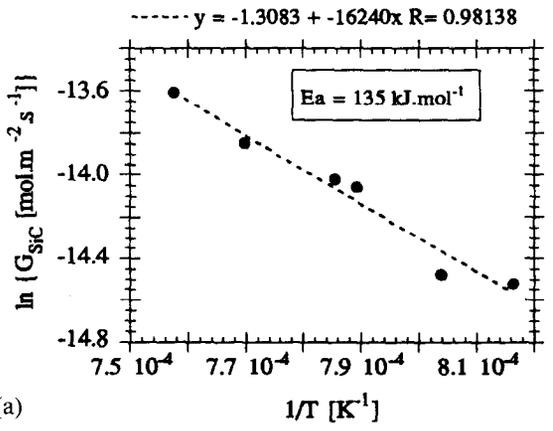

Fig. 14(a). The logarithmic SiC growth rate versus the reciprocal preform temperature; H_2/MTS = 5.

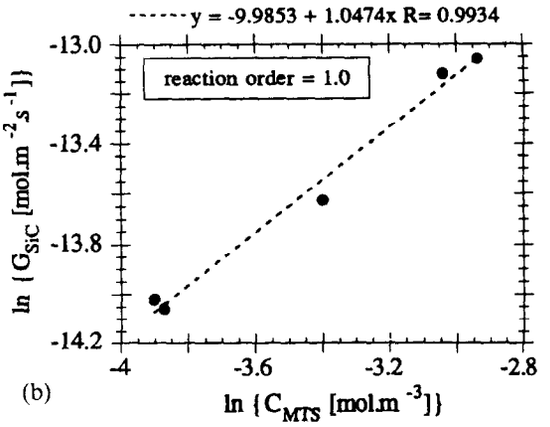

Fig. 14(b). The logarithmic SiC growth rate versus the logarithmic MTS concentration at input.

$$G_{SiC} = 16{\cdot}45 \exp\left(\frac{-135 \times 10^3}{T\ Rg}\right) C_{MTS}^{1{\cdot}0} \tag{13}$$

Because the experiments were performed at $DaI_{bed} < 0{\cdot}054$, it is assumed that surface kinetics have been dominating growth.

4.7 Effect of the shut off pressure drop on the infiltration time and composite density

The effect of the pressure difference across the preform (shut off point) on the infiltration time and the composite density was studied. The results are presented graphically in Figs 15 and 16.

After termination of the experiments, the permeability of the composite at the end of the process was calculated using eqn 5 at the pressure drop shut off point, temperature and gas composition used.

Initially, during the first 4 h of infiltration, the pressure drop across the preform hardly rises *viz.* from 0·13 to 1·2 kPa. After approximately 7 h, the injector pressure (and pressure drop) start rising rapidly, because the pores in the preform reach a critical size. Within approximately an hour the injector pressure rises from 5 to 55 kPa.

In this time lapse hardly any additional matrix is deposited within the small pores (Fig. 16). Here, not

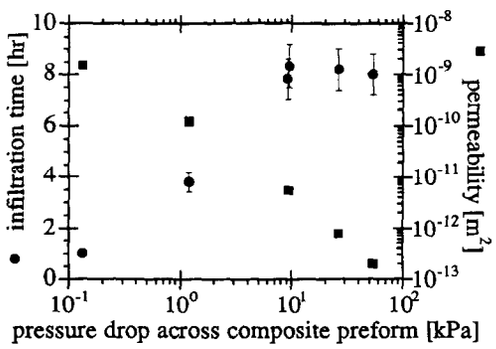

Fig. 15. The infiltration time and composites permeability versus shut off pressure difference. T = 1255 K, H_2/MTS = 6·00, V_f = 47·4 vol%, $Ft^{\#}$ = 2·49 × 10^{-5} m^3.s^{-1}, L = 2·90 × 10^{-3} m, p_L = 1·33 × 10^3 Pa, Pe_{bed} = 5·05 × 10^{-3}, DaI_{bed} = 3·97 × 10^{-2}–3·32 × 10^{-2}, A_{dep} = 6·54 m^2.

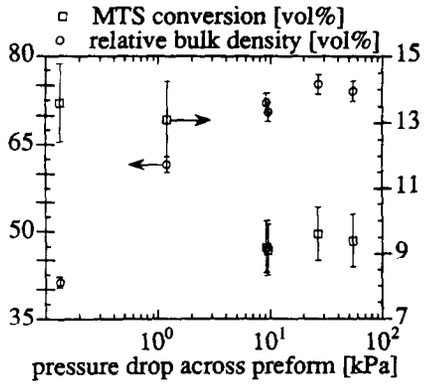

Fig. 16. The relative bulk density and MTS conversion versus pressure difference and infiltration time. T = 1255 K, H_2/MTS = 6·00, V_f = 47·4 vol%, $Ft^{\#}$ = 2·49 × 10^{-5} $m^3.s^{-1}$, L = 2·90 × 10^{-3} m, pL = 1·33 × 10^3 Pa, Pe_{bed} = 5·05 × 10^{-3}, DaI_{bed} = 3·97 × 10^{-2}–3·32 × 10^{-2}, A_{dep} = 6·54 m^2.

only density, but the uniformity expressed in terms of MTS conversion is also constant. It appears that a pressure drop of about 10 kPa is sufficient to reach maximum density at the selected infiltration conditions. Further densification will only yield a thicker coating on the gas inlet side of the sample.

The permeability of the composite is a decreasing function of the pressure drop. Even when composite density is not further enlarged, permeability still decreases. This drop in conductance for the gas flow will, however, be attributed to the deposited coating on the gas inlet side and narrowing of the pore mouth of the sample instead of the whole preform structure. At the point of just reaching maximum density, the permeability of the preform structure is decreased at least two orders of magnitude.

General remarks

The FCVI process can be represented as a two stage process in which both the small pores in a fibre bundle and the bigger pores inbetween the bundles have to be infiltrated. Convection is present in the big pores between the bundles (FCVI), whereas mass transport of the gaseous species into the bundles will be dominated by diffusion since there is no Δp from outer to inner volume of the bundle (this is in fact ICVI).

During the first hours of infiltration, the matrix deposits onto the available surface area and density increases rapidly (Fig. 16). Each filament is coated with a layer of SiC. As soon as a fibre bundle has grown together, the available surface area is greatly reduced and the larger pores between the bundles will become smaller. As a result, density gain is less rapid. During this time lap, a pressure increase is observed. As soon as the resistance for the gas flow is getting too big, the injector pressure increases very rapidly and the experiment is shut off.

5 General Discussion and Conclusions

The results presented above are consistent with the general concepts that are described in Part 1 of this study. For homogeneous densification, matrix growth within the kinetically limited growth regime is preferred. For rapid infiltration, forced convection should control matrix growth.[9]

Comparison with the FCVI model

The infiltration characteristics as a function of process variables were investigated and appear to qualitatively coincide with the FCVI model predictions of Part 1 of this study. Therefore, infiltration trends may be predicted using a 1D cylinder pore approach.

The transition point (x-value) of kinetically controlled towards convective controlled growth conditions of the model and of the experiments coincide (compare Fig. 5 Part 1 with Figs 3 and 4 Part 2, Fig. 7 Part 1 with Figs 5 and 6 Part 2, and Fig. 8 Part 1 with Figs 7 and 8 Part 2).

However, the effect of the preform temperature on the infiltration time as experimentally observed — in the kinetically limited growth conditions — is less pronounced than simulated with the model (Fig. 8 Part 1). The trend that the composite density is unaffected by temperature increase in the kinetically limited growth conditions is in agreement with model predictions. Increase of the total gas flow rate or decrease in outlet pressure — in the mass transport limited growth regime—yields an increase of the gas velocity and hence uniformity of the deposited SiC layer within the pores. The model (Figs 5 and 7 Part 1) and experimental observations are in agreement.

The MTS content in the gas mixture has no effect on the resulting composite density for both model and experiments. The increase of injector pressure with time as experimentally observed and calculated with the model (Fig. 3 Part 1) are in good agreement. Also, when infiltration proceeds densification is rapid initially, but levels off later on.

According to the model, high raw preform porosity yields low composite density. As such, experimental observations indicate the opposite. However, decrease of the raw preform porosity without affecting other microstructural parameters such as tortuosity, pore diameter, preform thickness and deposition area cannot be achieved. In terms of pore diameter, model (Fig. 6 Part 1) and experimental results do coincide.

Experimental observations

It appeared that a Peclet number (for a packed bed) larger than 4 × 10^{-3} corresponds with convective mass transport. $Pe_{bed} < 4 \times 10^{-3}$ and DaI_{bed}

$<5 \times 10^{-2}$ coincide with kinetically limited SiC growth conditions. The apparent overall reaction rate of the heterogeneous controlled conversion of MTS to SiC follows a first order dependence in MTS with an apparent activation energy of 135 kJ.mole^{-1}. The pre-exponential factor equals 16·45 m.s^{-1}.

In principle, for this first order reaction, low first Damköhler numbers and MTS conversion are in agreement with large IFCVI composite density. The highest composite density gained in this study was 75% of the ideal density at a MTS conversion smaller than 15%. Since the determination of the relative bulk density of the composite samples is subjected to many errors and its measurement is even impossible for complete geometries, the simple total MTS conversion appears to be a powerful tool in the estimation of the optimum process conditions.

It should be noted that the transition values of the Peclet and first Damköhler number itself should be treated with care. Their order of magnitude or moreover its transition value is very much dependent on the definition used, especially its characteristic length. The optimum pressure shut off point is dependent on the permeability of the raw preform. A poorly permeable preform structure requires a larger pressure drop to reach the same density as compared to a preform of large permeability. A constraint of the FCVI technique is that only preforms with high permeability without closed porosity are suitable to gain large composite density and strength. More generally stated, $LA^{-1}\ K^{-1}$ should be small.

Optimum infiltration, i.e. the largest density gain for a 80 mm diameter, 3 mm thick preform in the shortest time, occurs with a preform of 46 vol.% fibre, a temperature of 1320 K, outlet pressure of 6·65 kPa, total gas flow rate of 4×10^{-5} m^3.s^{-1}, MTS fraction of 16 vol.% and a pressure drop shut off point of 10 kPa. Clearly, these specific conditions are only applicable for preforms of exactly the same microstructure as the one studied and a first order heterogeneous decomposition reaction at the pore walls.

In general, high composite density is reached at IFCVI conditions of kinetically controlled matrix growth and hence implies: high total gas flow rate, low preform temperature, low outlet pressure, arbitrary precursor fraction in the gas mixture, high pressure shut off difference, low raw preform fibre content and high raw preform gas permeability. A negative effect of the initial pressure drop ($t = 0$) on the composite density was not observed at least as long as $p_0/p_L < 1{\cdot}6$. On the other hand, rapid IFCVI is achieved at mass transport limited matrix growth conditions and generally at: high total gas flow rate, high preform temperature, high outlet pressure, high precursor fraction in the gas mixture, low pressure shut off difference, high raw preform fibre content and low raw preform gas permeability.

Unfortunately, these two criteria — with the exception of the total gas flow rate and MTS fraction in the gas — obviously are contradictory. It should be noted that again a too large gas velocity — typically $u_{bed} > 3$ m.s^{-1} — can lead to poor infiltration, because the residence time of the MTS precursor in the preform is insufficient to cause a deposition reaction at its fibre surface.

References

1. Roman, Y. G., Kotte, J. F. A. K. & de Croon, M. H. J. M., *J. Eur. Ceram. Soc.*, **15** (1995) 875–86.
2. Schlichting, J., *Powder Metallurgy International*, **12** (1980) 141–200.
3. Patent DASA: in preparation.
4. Collins, R. E., *Flow of fluids through porous materials*, Reinhold Publ. Corp. New York, Ed. C. R. Wilke (1961).
5. Scheidegger, A. E., *The physics of flow through porous media*. University of Toronto Press, 1957.
6. Philipse, A. P. & Schram, H. L., *J. Am. Ceram. Soc.*, **74** (1991) 728–32.
7. Kaviany, M., *Principles of heat transfer through porous media*, Springer Verlag, 1991.
8. Burgess, J. N. & Lewis, T. J., *Chem. and Ind.*, **19** (1974) 76–7.
9. Roman, Y. G., Forced flow Chemical Vapour Infiltration, PhD Thesis Eindhoven University of Technology, Eindhoven, The Netherlands (1994).